CHAPTER 5 – SECONDARY MINERALS IN THE LHZBG AND PCR UNITS

5.1 Amphibole

The amphiboles found in the Uitkomst (Figure 5.1) samples are secondary in nature, replacing the original primary mineralogy during retrograde metamorphism of the mafic rocks as well as dolomite. Some pyroxene grains, especially in the LHZBG, have been entirely replaced by fibrous amphibole and may be referred to as uralitized grains. Uralite is the term used to describe the conversion of pyroxene to secondary fibrous amphibole of uncertain composition (Deer et al., 1992). The process of uralitization is ascribed to the action of hydrothermal solutions which may be associated with late stage crystallization of igneous rocks or due to metamorphism or metasomatism (Deer et al., 1992).

5.1.1 Amphiboles of the LHZBG Unit

Amphiboles are the dominant minerals in the LHZBG Unit. These amphiboles (actinolite, tremolite etc.) are less magnesium-rich than amphibole samples of the PCR Unit. Parts of the LHZBG have been altered to such an extent in the boreholes investigated that the entire matrix of the sample is composed of amphibole and the rock type may then be is referred to as amphibolite. Amphiboles in the LHZBG Unit are associated with or replace clinopyroxene grains and are associated with chlorite and brown phlogopite. Some of the uralitized grains also appeared to be pseudomorphic after olivine grains. In borehole UK61, hornblende and tremolite occur in association with dolomite and talc. The sulphide minerals tend to have sharp contacts with the amphibole grains, especially the hornblende grains. Some of the sulphide grains are intergrown with tremolite blades.

5.1.2 Amphiboles of the PCR Unit

The amphiboles (hornblende, magnesio-gedrite, magnesio-cummingtonite etc.) of the PCR unit are very magnesium-rich in composition, with the exception of the PCR unit intercepted in borehole UK12 (sample UK12D), which is located in the narrow part of the intrusion. The grains forming the matrix of these samples are anhedral and some of these grains have pockets of chlorite within them. A few samples are composed completely of amphibole and

chlorite. The amphibole in sample UK48C is associated with remnants of olivine, which are totally serpentinized, containing secondary magnetite. Amphiboles rimming the sulphide minerals are also very magnesium-rich and tend to protrude into the sulphide grains.

5 5.1.3 Microprobe analyses results of amphibole grains

Table 5.1 presents the amphiboles associated with each of the sections that was analysed. The results of the microprobe analyses and mineral formulas are presented in Appendix 2.

Table 5.1 Amphibole minerals in the PCR and LHZBG Units.

Borehole	Unit	Magnesio-anthophyllite	Magnesio-gedrite	Magnesio-cummingtonite	Tremolite	Tremolitic-hornblende	Magnesio-hornblende	Hornblende	Actinolite	Actinolitic-hornblende	Tschermakite	Pargasite-hornblende	Pargasite	Edenite	Edenitic-hornblende	Magnesio-hastingsite
UK12D	PCR							x								
UK12G	PCR		x	x			x					x				x
UK48C	PCR		x	x												
UK48G	PCR			x												
UK48I	PCR	x						x								
UK61A	PCR	x	x	x			x				x					
UK61B	PCR				x											
UK61C	PCR		x	x												
UK12H	LHZBG		x	x			x								x	
UK12J	LHZBG					x					x			x		x
UK12L	LHZBG												x			x
UK48L	LHZBG				x										x	
UK48N	LHZBG				x				x							
UK61E	LHZBG				x	x			x	x						
UK61F	LHZBG	x	x	x												

Microprobe analyses of amphibole grains, presented in Appendix 2, were recalculated and averaged before being plotted. This yields the results presented in figures 5.2 to 5.15.

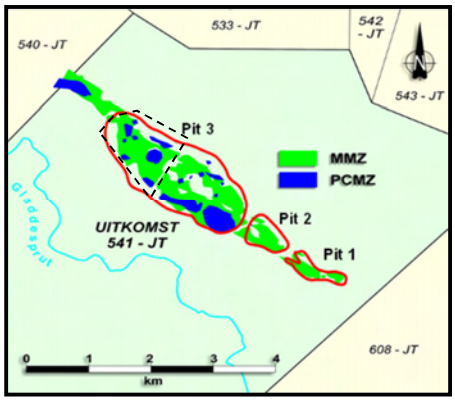

Figure 5.1. Study area located in upper left hand side of pit 3 (black dash line). Figure courtesy Nkomati Mine geological staff.

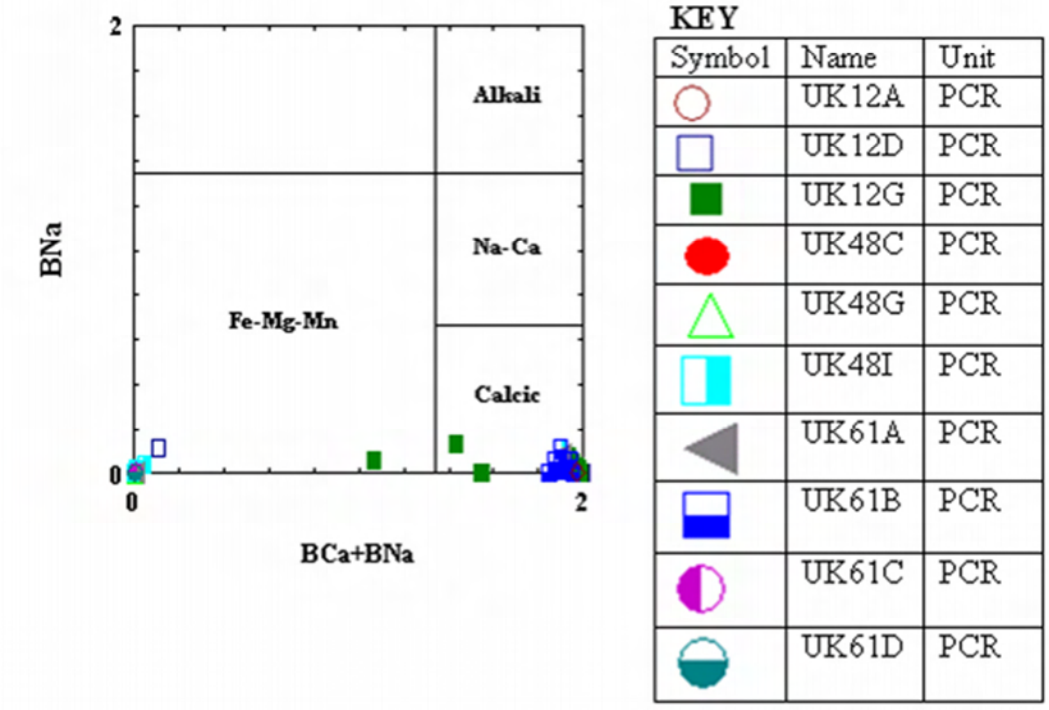

Figure 5.2. Classification diagram for the four principal groups of amphiboles in the PCR Unit (After Hawthorn, 1981).

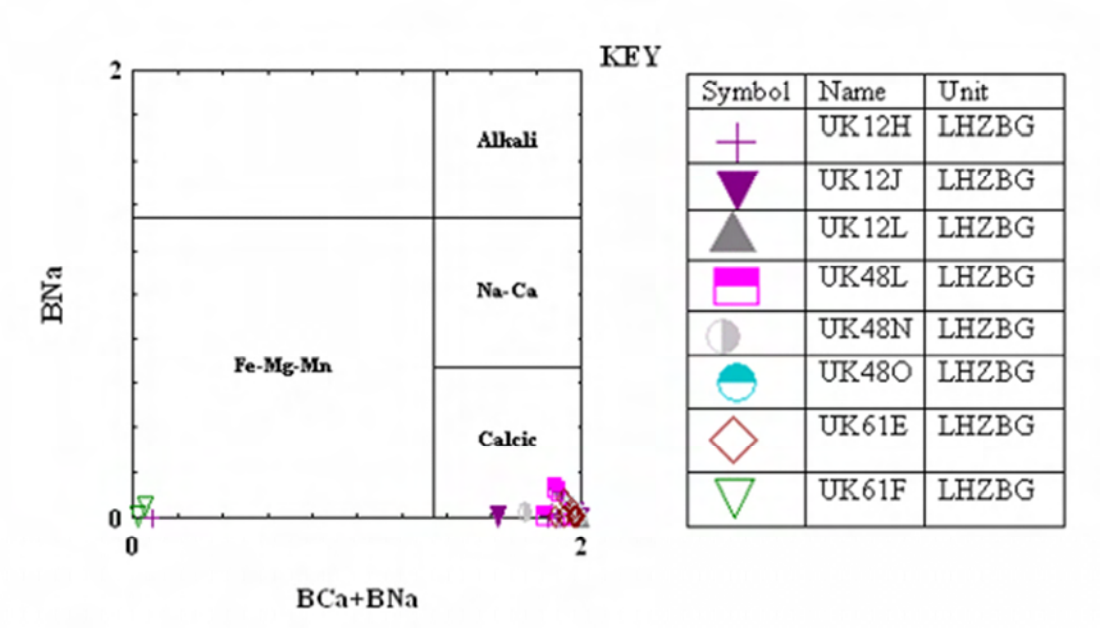

Figure 5.3. Classification diagram for the four principal groups of amphiboles in the LHZBG Unit (After Hawthorn, 1981).

By plotting the recalculated analyses according to Na in the B-position against Ca and Na in the B-position, it is shown that most of the amphiboles are calcic, with some Fe-Mg-Mn amphiboles also being present (Figures 5.2 and 5.3). This correlates with van Zyl's (1996) findings. The dominance of calcic amphiboles may indicate the accommodation of Ca into amphibole species, after assimilation of the dolomitic country rock.

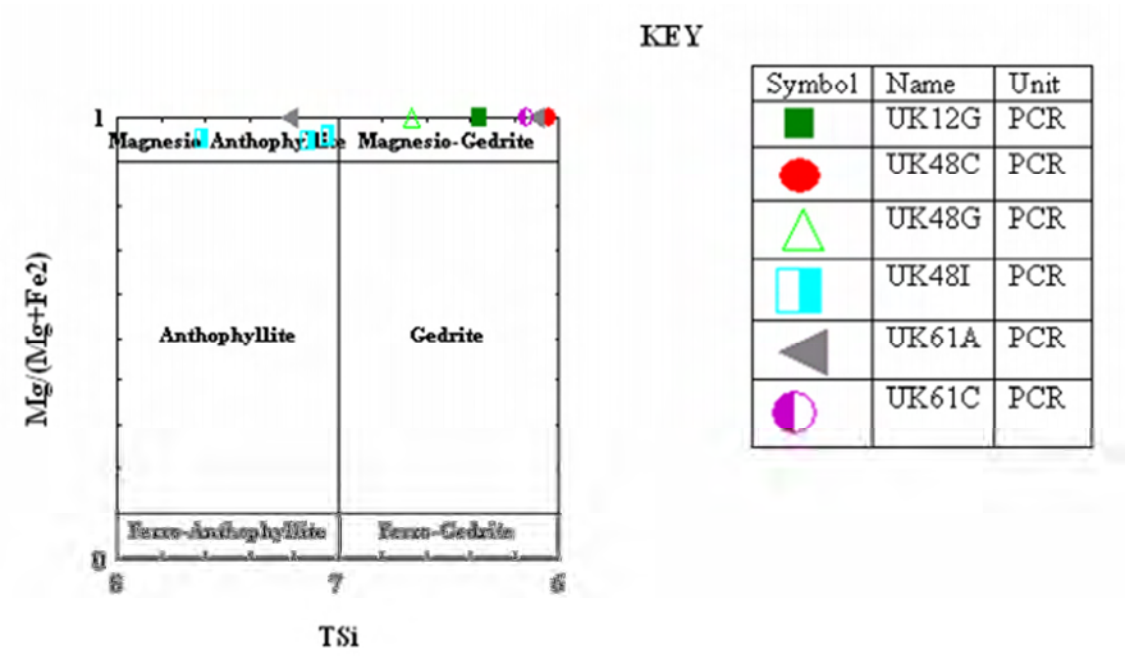

Figure 5.4. Classification diagram for Fe-Mg-Mn group orthorhombic amphiboles in the PCR Unit (After Hawthorn, 1981).

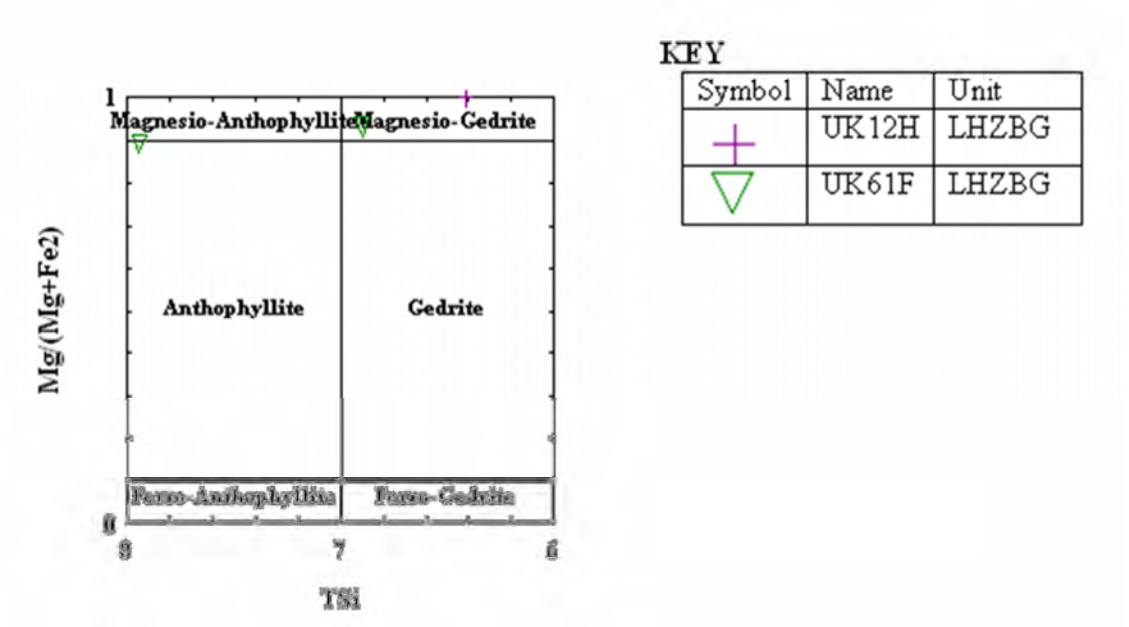

Figure 5.5. Classification diagram for Fe-Mg-Mn group orthorhombic amphiboles in the LHZBG Unit (After Hawthorn, 1981).

According to Deer et al., (1992) orthorhombic amphiboles are unknown in igneous rocks. Anthophyllite and gedrite do however occur in metamorphic and metasomatised rocks, and these minerals are also commonly found in the reaction zone between ultramafic rocks and country rocks. These two minerals (presented in Figure 5.4 and 5.5) may also develop during lower amphibolite facies conditions (Deer et al., 1997). Orthoamphiboles may be derived from calcic amphiboles by metasomatism, e.g. hornblende or actinolite, in the latter due to hydrothermal alteration involving the addition of Mg and the loss of Fe, Ti and Ca (Deer et al., 1997). The formation of anthophyllite may also be due to the addition of Fe, Mg or Al and the removal of Ca during metamorphism (Deer et al., 1992). Anthophyllite commonly occur as an alteration product in rocks rich in olivine (Deer et al., 1997). Anthophyllite may also form due to retrograde metamorphism of earlier thermally metamorphosed rocks (Deer et al., 1992).

Magnesio-antophyllite and magnesio-gedrite is found in both the PCR (Figure 5.4) and LHZBG (Figure 5.5) Units. Less evidence of magma-country rock interaction exists in the PCR Unit relative to the LHZBG Unit, thus the possibility of it representing an interaction product is considered unlikely. Samples UK12H and UK61F, from the LHZBG (Figure 5.5) Unit, contain magnesio-antophyllite and magnesio-gedrite. This probably represents interaction between the intruding ultramafic magma and the surrounding dolomitic country rock.

The relict poikilitic texture of the PCR Unit is shown in Figure 5.6. In this unit, magnesio-anthophyllite is found in association with serpentine, likely representing alteration of the precursor mafic minerals orthopyroxene (enstatite) and olivine respectively. Magnesio-gedrite and –anthopyllite is found in PCR samples: UK12G, 48C, 48G, 48I, 61A and 61C (Figure 5.4).

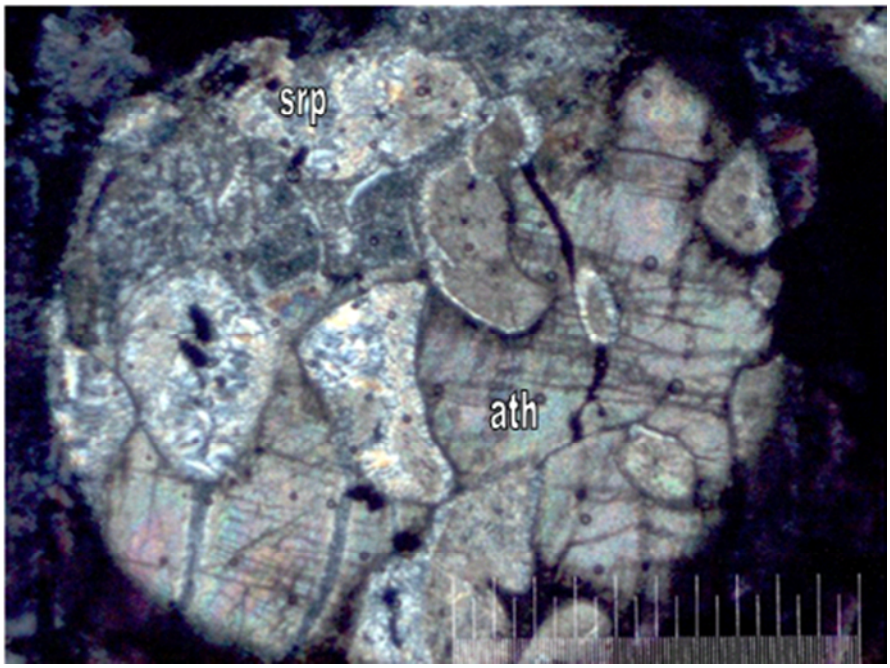

Figure 5.6. Relict pokilitic texture in the PCR Unit. Serpentinised (srp) grains (top left, higher birefringence) probably after olivine and magnesio-anthophyllite (ath) (bottom right, low birefringence) probably after Mg-rich orthopyroxene grains from the PCR. The picture scale bar is 1000 micron. Taken with cross-polarised light. (Sample; UK48I).

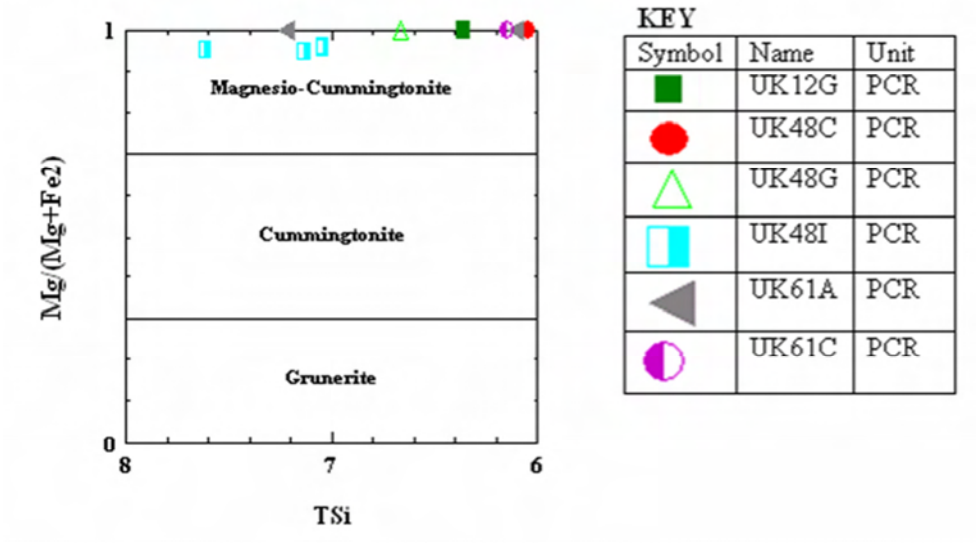

Figure 5.7. Classification diagram for Fe-Mg-Mn Group Monoclinic amphiboles in the PCR Unit (After Hawthorn, 1981).

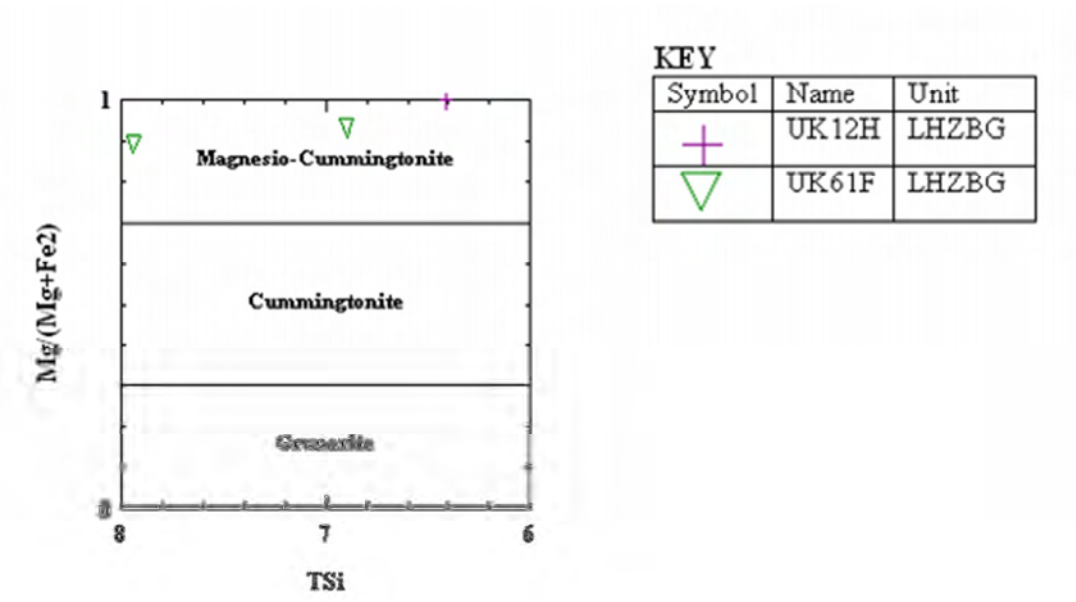

Figure 5.8. Classification diagram for Fe-Mg-Mn Group Monoclinic amphiboles in the LHZBG Unit (After Hawthorn, 1981).

According to Deer et al., (1992) magnesium-rich cummingtonite occurs together with anthophyllite in isochemically metamorphosed ultrabasic rocks. Cummingtonite is also found in hybrid rocks of intermediate composition and may occur as the middle member in the transition of orthopyroxene to hornblende (Deer et al., 1992).

The composition of the Uitkomst samples (magnesio-anthophyllite, magnesio-gedrite and magnesio-cummingtonite) may indicate that the samples represent ultrabasic rocks that suffered metamorphism and metasomatism. The magnesio-cummingtonite samples derived from the PCR Unit, and presented in Figure 5.7, are: UK12G, UK48C, G and I, UK61A, and C. Magnesio-cummingtonite also occurs at the top of the LHZBG Unit (UK12H) and middle (UK61F) of the unit (Figure 5.8). The greater abundance of magnesio-amphiboles in the PCR Unit relative to the LHZBG Unit may indicate the magma that formed the PCR Unit may have been more primitive than the magma that formed the LHZBG Unit or may have suffered less contamination by the dolomite country rock. It is also important to note

that the samples that contain magnesio-cummingtonite are the same samples that contain magnesio-anthophyllite and magnesio-gedrite (Figures 5.4 and 5.5).

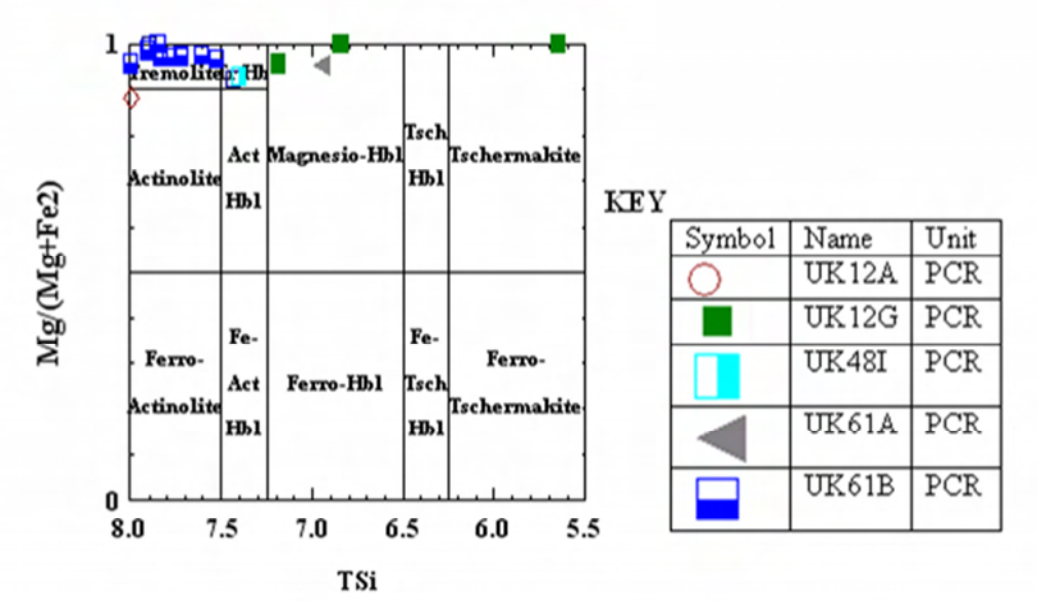

Figure 5.9. Classification diagram for the calcic group of amphiboles where ANa+AK<0.5;Ti<0.5 in the PCR Unit (After Hawthorn, 1981).

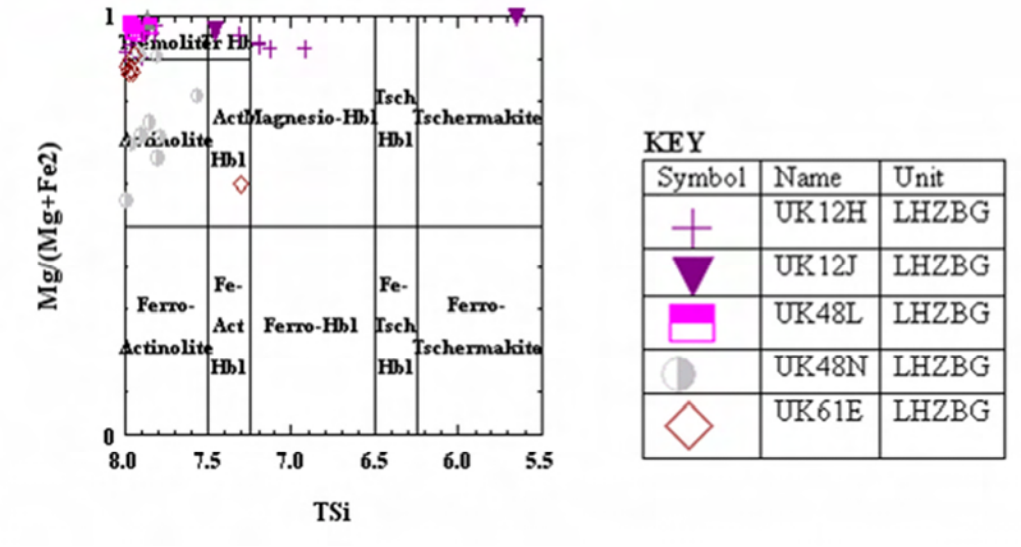

Figure 5.10. Classification diagram for the calcic group of amphiboles where ANa+AK<0.5;Ti<0.5 in the LHZBG Unit (After Hawthorn, 1981).

Tremolite and actinolite are metamorphic minerals that may occur in both contact and regionally metamorphosed rocks. Actinolite is a common product of retrograde metamorphism of ultrabasic rocks. Actinolite usually develops in pyroxene-rich rocks as an alteration product of both orthopyroxene and clinopyroxene (Deer et al., 1997). In ultrabasic rocks actinolite is usually associated with assemblages of tremolite-talc and or tremolite-carbonate-antigorite (Deer et al., 1997).

During thermal metamorphism of impure dolomites, tremolite forms early on in the reaction between dolomite and quartz by the reaction:

$$5CaMg(CO_3)_2 + 8SiO_2 + H_2O = Ca_2Mg_5Si_8O_{22}(OH)_2 + 3CaCO_3 + 7CO_2$$

Tremolite forms at the expense of talc and calcite (Provoden, Horacek and Abart, 2002). The reaction for the formation of tremolite as a result of this is:

$$1.5x\ \text{Calcite} + 1x\ \text{Talc} = 0.5x\ \text{Dolomite} + 0.5x\ \text{Tremolite} + 0.5x\ H_2O + 0.5x\ CO_2$$

With increasing metamorphic grade, tremolite becomes unstable, and, in the presence of silica and calcite, tremolite will react to form diopside (Deer et al., 1997). Where quartz has been exhausted, the remaining dolomite will react with tremolite to produce fosterite and calcite. Both of these reactions liberate CO_2 and H_2O, but the temperature of reaction will depend on the fluid volume and composition. These reactions do not appear to have occurred in the Uitkomst Complex, as the olivine has been found only as a magmatic phase. The tremolite-actinolite-hornblende assemblages (Figure 5.10) are present in the middle (UK12J and UK48N) to upper parts of the LHZBG Unit (UK12H, UK48L and UK61E) as depicted in Figure 5.10 and in the upper parts of the PCR Unit (UK12D, UK61A and B) and bottom part of the PCR (UK12G) as depicted in Figure 5.9. Amphiboles of this composition are occasionally intergrown with sulphide grains.

Tremolite is the dominant amphibole mineral found in the LHZBG Unit, in the Uitkomst Complex, on the farm Slaaihoek 540 - JT (Steenkamp, 2004). The Slaaihoek samples appeared more pristine relative to samples from the current study area. In the Slaaihoek samples the tremolite pseudomorphically replaces pyroxene and olivine. Steenkamp (2004) also describe hybrid rocks that consist predominantly of tremolite and classify them as amphibolites.

The occurrence of the actinolite-tremolite in the middle- and upper parts of the LHZBG Unit (Figure 5.10) and lower part of the PCR Unit (Figure 5.9) may indicate that the H_2O-rich fluid migrated upward and affected the minerals above and below the contact between the two units. In contrast, the abundance of actinolite-tremolite only again in the upper part of the PCR may indicate that the H_2O-rich fluid was trapped below the MCR Unit developed on the contact between the PCR and MHZBG Units.

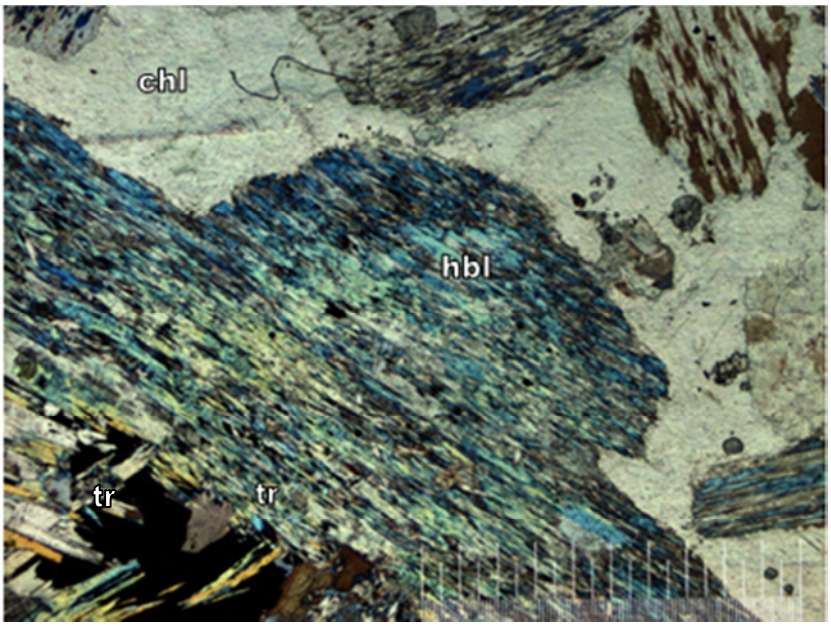

Figure 5.11. Diopside grains entirely replaced by tremolite (tr), magnesio-hornblende (hbl) (acicular grains, high birefringence) in centre of view. Chlorite (chl) is associated with the tremolite and magnesio-hornblende grains and forms the surrounding matrix material. Tremolite also protrudes into a sulphide grain (black, bottom left). The picture scale bar is 1000 micron. Taken with cross-polarised light. (Sample: UK12H).

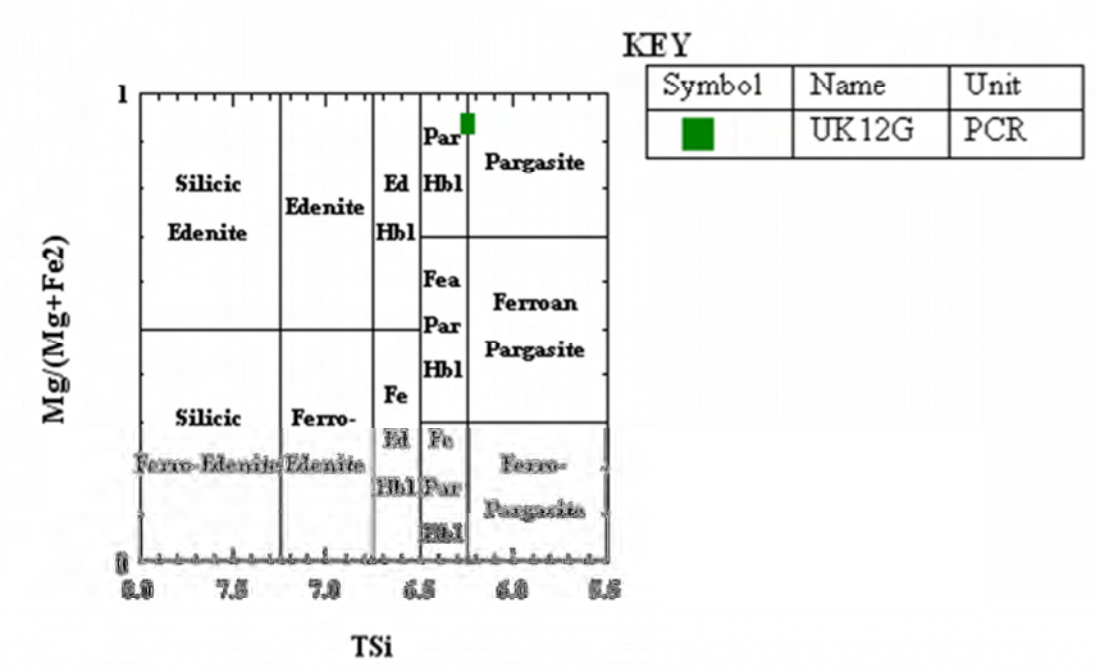

Figure 5.12. Classification diagram for the Calcic Group of amphiboles where Ana+AK>0.5;Ti<0.5;Fe3<Alvi in the PCR Unit (After Hawthorn, 1981).

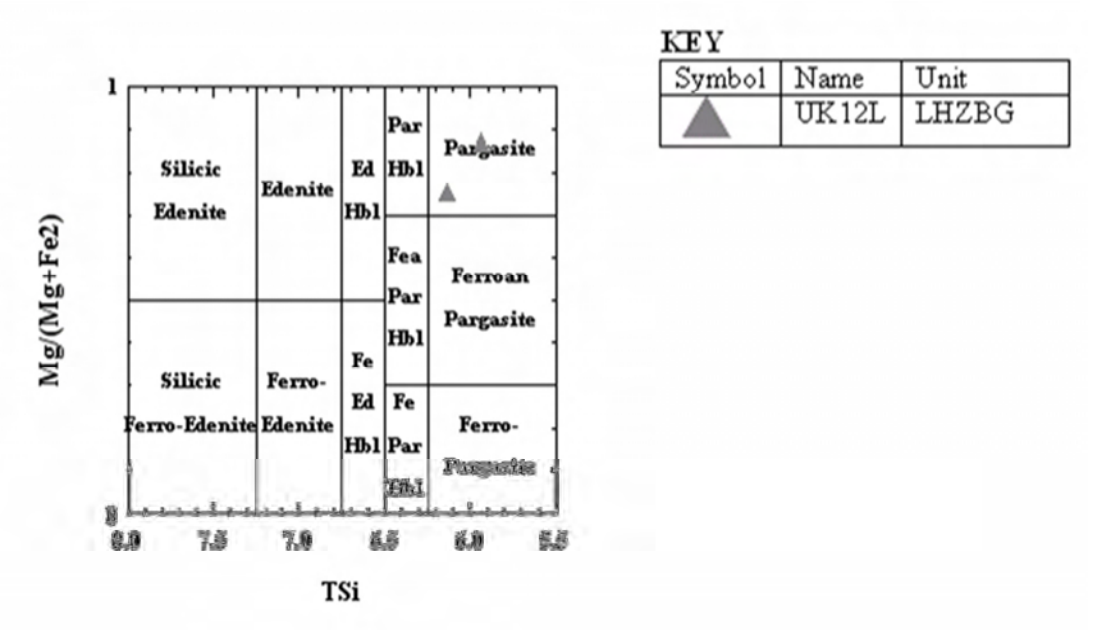

Figure 5.13. Classification diagram for the Calcic Group of amphiboles where Ana+AK>0.5;Ti<0.5;Fe3<Alvi in the LHZBG Unit (After Hawthorn, 1981).

Pargasite-hornblende and pargasite also occur in metamorphosed impure dolomites and limestone (Deer et al, 1992). The composition of hornblende and pargasite is sensitive to pressure and temperature, but this relationship is affected by the bulk rock composition, fluid phase and the oxygen fugacity (Deer et al., 1997).

Pargasite is found only in sample UK12G from the lower part of the PCR Unit and in sample 12L from the lower part of the LHZBG Unit. This may indicate xenolithic material of metamorphosed impure dolomitic material is associated with the samples from the narrower part of the intrusion. This may represent finger structures of penetrating or preserved country rock in the narrow part of the intrusion in the study area.

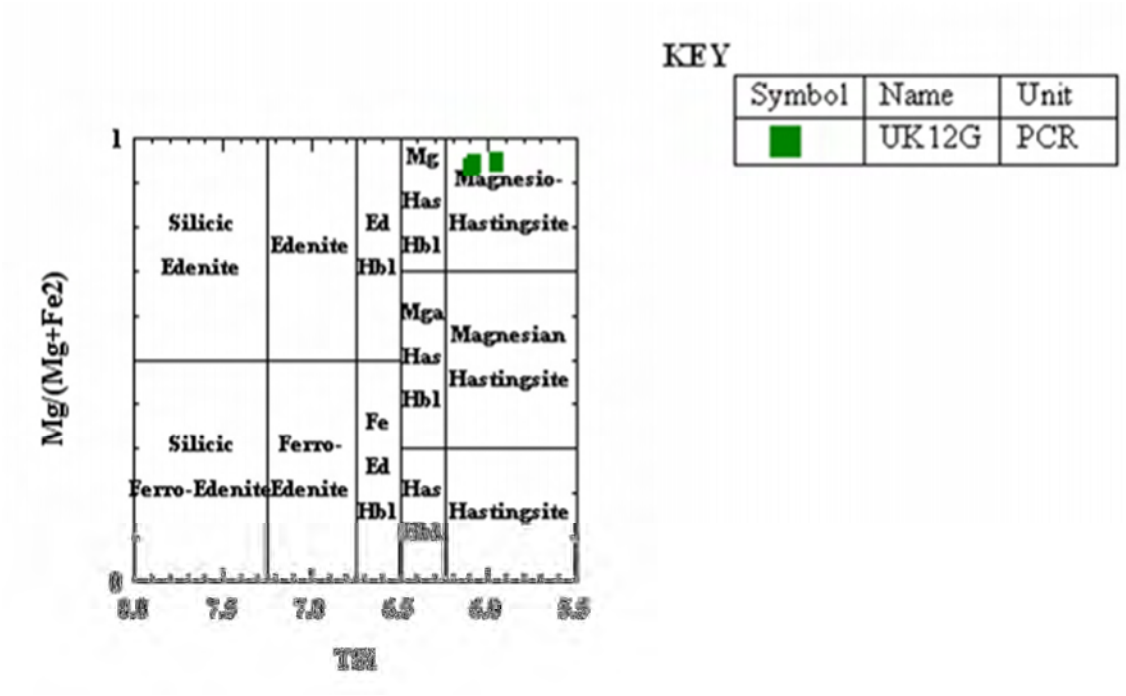

Figure 5.14. Classification diagram for the Calcic Group of amphiboles where ANa+AK>0.5;Ti<0.5;Fe3>Alvi in the PCR Unit (After Hawthorn, 1981).

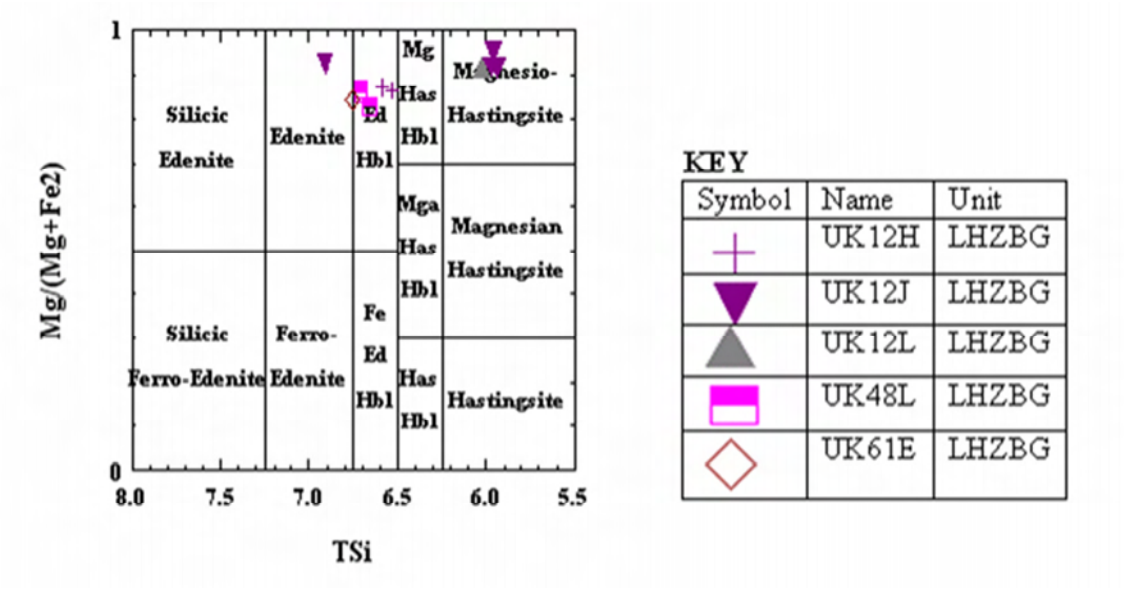

Figure 5.15. Classification diagram for the Calcic Group of amphiboles where ANa+AK>0.5;Ti<0.5;Fe3>Alvi in the LHZBG Unit (After Hawthorn, 1981).

According to Deer et al., (1992), the wide range of chemical substitution possible in hornblende leads to its existence in a wide variety of igneous and metamorphic petrogenetic conditions. Magnesio-hastingsite usually only occurs in alkali basalt and calc-alkaline rock (Deer et al., 1992). In andesitic rocks hornblende is usually accompanied by olivine and has been suggested to form due to interaction between olivine and the andesitic fluid (Deer et al., 1992). It was suggested by de Waal et al. (2006) that the edenite and magnesio-hastingsite amphiboles found in the high-Ti suite samples stabilized after clinopyroxene in the paragenetic sequence, and its concentrations are directly proportional to the amount of trapped liquid. It was indicated by Arndt et al. (2005) that the presence of H_2O and CO_2 in magma will manifest mineralogically as phlogopite and magmatic amphibole in the groundmass.

The magnesio-hastingsite mineralization in the Uitkomst Complex is found in the lower and middle part of the LHZBG Unit (Figure 5.15) and the lower parts of the PCR Unit (Figure 5.14) in the narrow part of the intrusion. Edenite-hornblende, also indicated in Figure 5.15, is found in the upper part of the LHZBG Unit in all three of the analysed boreholes. The

only edenite (Figure 5.15) found is in the middle part of the LHZBG Unit in the narrow part of the intrusion. Pargasite, magnesio-hastingsite and edenite are in contact with, but are not intergrown with sulphide grains.

Following de Waal et al. (2006), it is suggested that the magnesio-hastingsite and edenite-hornblende may represent amphiboles formed as part of the paragenetic sequence of mineralization of the magma due to trapped liquids. This hypothesis is supported by the presence of the magnesio-hastingsite and edenite in proximity to preserved olivine grains (Figure 5.16). The magnesio-hastingsite, edenitic-hornblende and edenite are also found in greater abundance in the LHZBG Unit relative to the PCR Unit, suggesting more interaction with trapped fluids in the LHZBG Unit. The magnesio-hastingsite found in the PCR Unit comes only from sample UK12G, the lower part of the PCR Unit. This may suggest interaction with trapped fluids took place only in the lower part of the PCR Unit, in the narrower part of the intrusion in the study area.

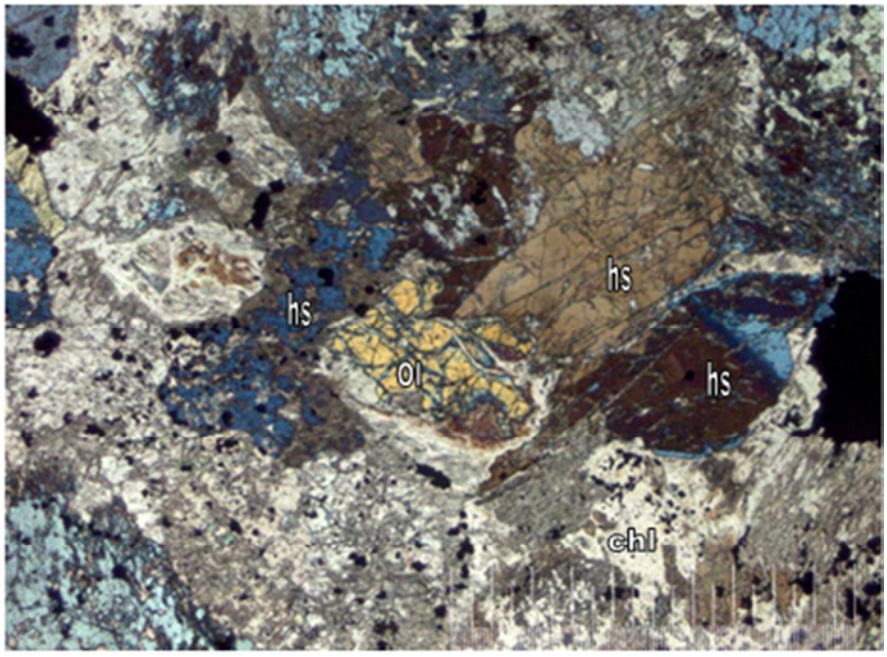

Figure 5.16. Olivine (ol) (yellow grain, centre of view), magnesio-hastingsite (hs) (light brown grain, to top right of olivine) and the combination blue-brown grains are mainly magnesio-hastingsite (hs) with minor edenite (ed). The low birefringence mineral is chlorite (chl). The black mineral is a sulphide grain. The picture scale bar is 1000 micron. Taken with cross-polarised light. (Sample: UK12J).

5.2 Chlorite

Chlorite is a secondary mineral that forms due to deuteric or hydrothermal alteration of primary ferromagnesian minerals such as mica, pyroxenes, amphiboles, garnets and olivines at temperature of up to 400 ˚C (Deer et al., 1992). The composition of the chlorite is often related to that of the original minerals, but the ideal formula of chlorite is (Mg, Fe^{2+}, Fe^{3+}, Mn, Al)$_{12}$[(Si,Al)$_8$O$_{20}$](OH)$_{16}$ (Deer et al., 1992).

Chlorite is found in the all of the analysed (XRD) samples of the BGAG, LHZBG and PCR Units. In the PCR Unit the chlorite has a white-green colour. In some instances, chlorite and talc form the entire matrix (e.g. UK12A). Chlorite also occurs in association with serpentine and talc (e.g. UK48G). Chlorite and amphibole also occur together in relic dolomite grains (UK61C) along with talc (e.g. UK61F). Chlorite in the LHZBG Unit appears green-white to white. Here it is associated with amphibole and is present as pockets within amphibole (e.g. UK12J presented in Figure 5.17) and diopside. Chlorite also forms part of rims surrounding sulphide grains, but the sulphides are not intergrown by the chlorite.

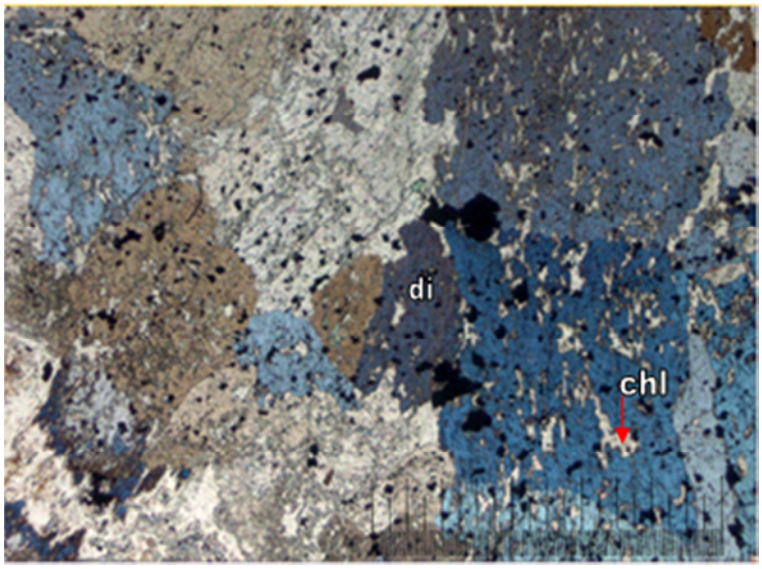

Figure 5.17. Pockets of chlorite (chl) (off-white) in diopside (di) grains (blue and brown) with associated subhedral pyrite (black) grains form the Lower Harzburgite Unit. Note the triple junctions between the diopside grains. The picture scale bar is 1000 micron.Taken with cross-polarised light. (Sample: UK12J).

The average chlorite content (based on semi-quantitative XRD analyses) is 17 wt% in the BGAB Unit, 19 wt% in the LHZBG Unit and 21.6 wt% in the PCR Unit. This shows a progressive increase in chlorite content with stratigraphic height in the lower part of the Complex. Microprobe analyses of chlorite are provided in Appendix 2. The data was recalculated and plotted using *MinPet* software.

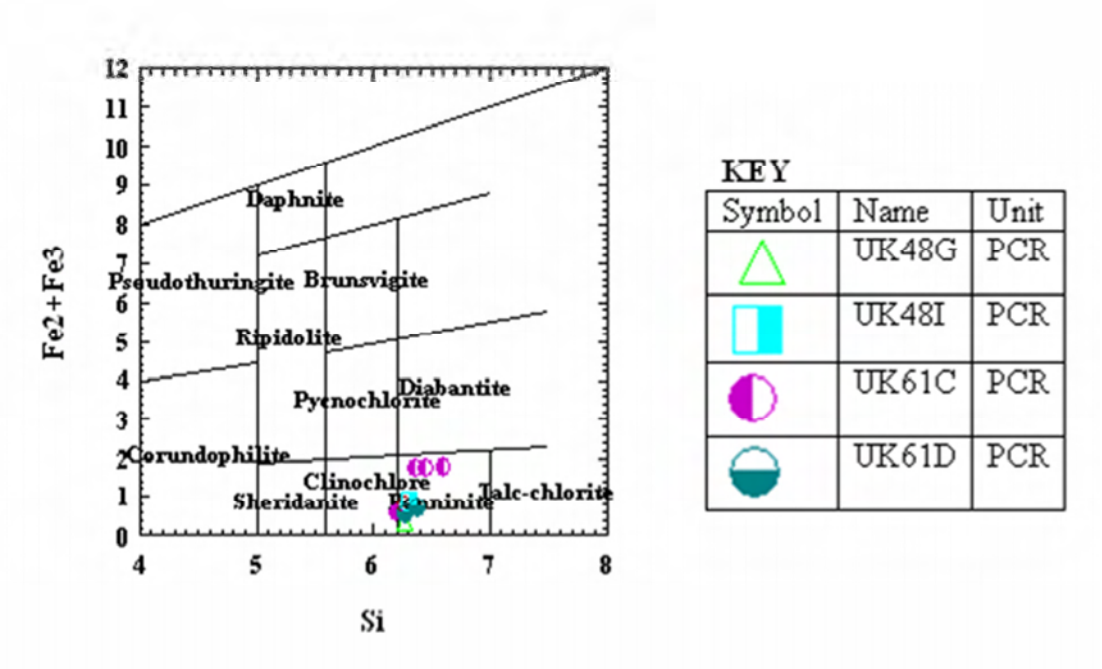

Figure 5.18. Chlorite classification diagram of Deer et al. (1972) showing chlorite grains analysed in the PCR Unit.

Using the classification scheme proposed, for the chlorite grains analysed, it may be seen that the chlorite composition fall mainly into the clinochlore, pycnochlorite and penninite composition range. Penninite is a manganese chlorite and clinochlore is an Mg-rich chlorite (Deer et al., 1992).

In the PCR Unit (Figure 5.18) all of the analysed chlorite grains fall in the penninite compositional range. In the LHZBG Unit (Figure 5.19) the chlorite composition range is

highly varied. The chlorite species in the LHZBG Unit are talc-chlorite, penninite, clinochlore, pycnochlorite and diabantite. The chlorite found in the xenoliths from the LHZBG Unit (Figure 5.20) falls in the ranges of clinochlore and pycnochlorite.

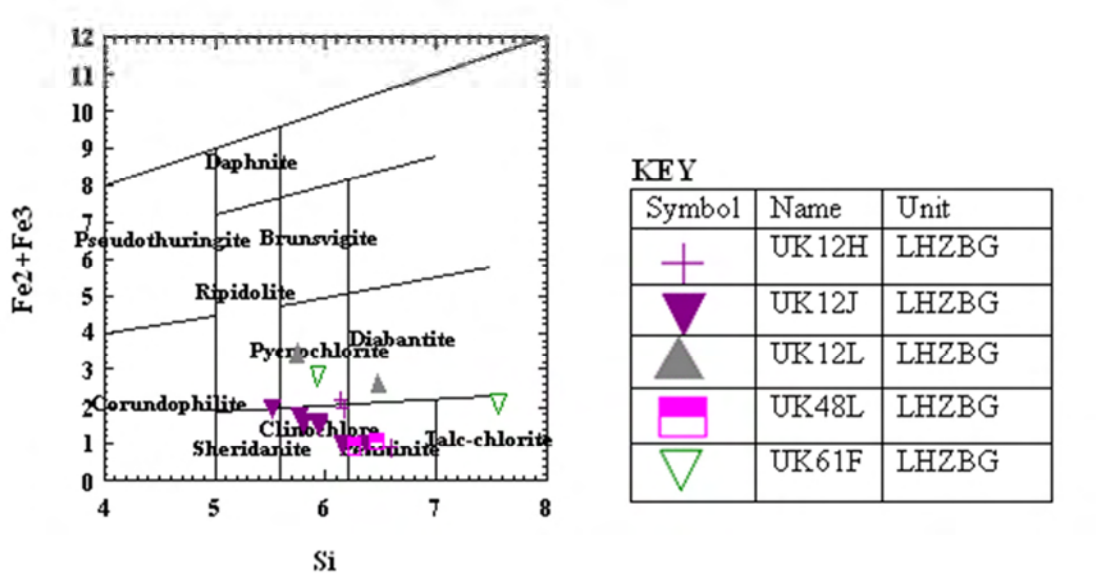

Figure 5.19. Chlorite classification diagram of Deer et al. (1972) showing chlorite grains analysed in the LHZBG Unit.

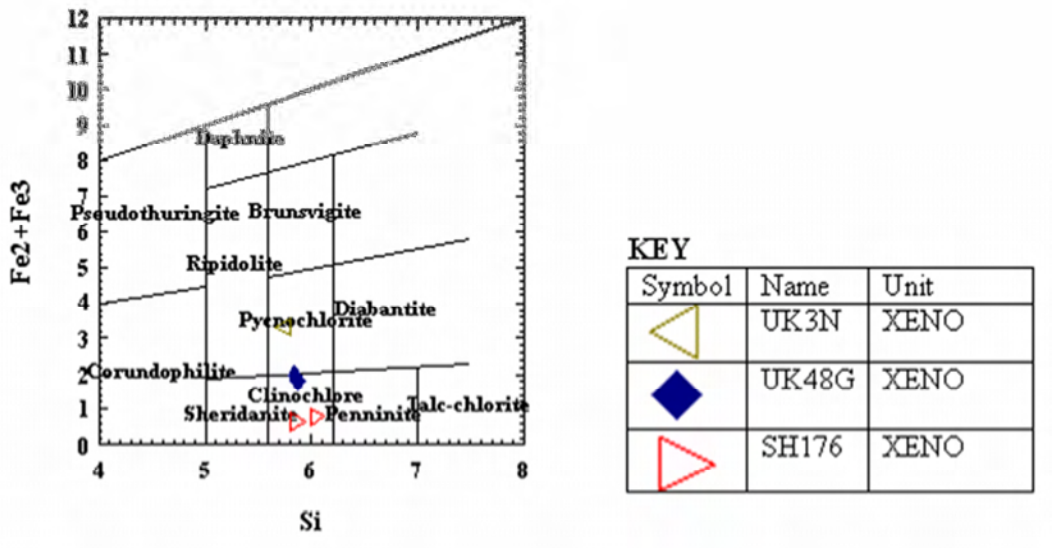

Figure 5.20. Chlorite classification diagram of Deer et al. (1972) showing chlorite grains analysed in the xenoliths from the LHZBG Unit.

The occurrence of the different species of chlorite is presented in Table 5.2

Table 5.2. Classification of chlorite in the different units.

Borehole	Unit	Pycnochlorite	Clinochlore	Penninite	Ripidolite	Diabantite	Talc-chlorite
UK12H	LHZBG	X	X	X			
UK12J	LHZBG		X		X		
UK12L	LHZBG	X				X	
UK48G	PCR			X			
UK48I	PCR			X			
UK48L	LHZBG			X			
UK61C	PCR			X			
UK61D	PCR			X			
UK61F	LHZBG	X					X
SH12H	XENO		X				
UK44G	XENO		X				

Chlorite in the calc-silicate xenoliths from the LHZBG Unit is of a clinochlore composition and those in the LHZBG are pycnochlorite, and clinochlore, with the exception of sample UK48L from the LHZBG Unit where the chlorite compositions plot predominantly in the penninte field. The chlorite from all samples of the PCR Unit, has the composition of penninite. These findings differ from those of van Zyl (1996) who found that the chlorite compositions are only of a pycnochlorite-diabantite composition.

The average compositions of chlorite from the LHZBG, PCR and xenoliths form the LHZBG Units are presented in Table 5.3. The results and calculated formulas are presented in Appendix 2.

Table 5.3. The average chlorite composition in the PCR, LHZBG and xenoliths from the LHZBG Units.

PCR	Al_2O_3	FeO	MnO	MgO
Mean	15.28	7.89	0.05	30.61
Std Dev	1.04	3.42	0.04	2.40
LHZBG				
Mean	17.46	11.79	0.23	25.85
Std Dev	2.19	4.67	0.13	4.44
Xeno				
Mean	19.63	10.54	0.56	24.65
Std Dev	0.77	5.56	0.23	3.85

The Al- and Mn content in the chlorite present in the xenoliths from the LHZBG Unit is the highest amongst the sampled rocks. The chlorite in the LHZBG Unit has the highest Fe content and the chlorite from the PCR Unit has the highest Mg content. The chlorite from the LHZBG Unit and the xenoliths from the LHZBG Unit have near similar composition, but differ notably from the composition of chlorite from the PCR Unit.

5.3. Serpentine

Retrograde metamorphism of ultramafic rocks requires the presence of H_2O and or CO_2. The most common hydrothermal alteration product of olivine is the serpentine mineral lizardite with pseudomorphic textures, with or without brucite, magnesite and magnetite. Serpentine is only stable at very low values of X_{CO_2}, which implies that the fluid phase that dominated at the time of its formation contained very little CO_2. The X_{CO_2} must be <10 mole%, otherwise serpentine would be converted to magnesite and quartz or talc (Winkler, 1974; Bucher-Nurminen, 1982; Provoden et al., 2002).

Of importance are the following reactions that take place at extremely low concentrations of CO_2 (Winkler, 1974):

1) 1 Serpentine + 1 magnesite = 2 fosterite + 2 Water + $1CO_2$
3) 2 Serpentine + 3 CO_2 = 1 talc + 3 magnesite + $3H_2O$
5) 1 Serpentine + 3 CO_2 = 2 quartz + 3 magnesite + $2H_2O$
6) 1 Serpentine + 1 brucite = 2 fosterite + $3H_2O$

7) 5 Serpentine = 6 fosterite + 1 talc + $9H_2O$

8) 1 Serpentine + 2 quartz = 1 talc + $1H_2O$

19) 1 Brucite +$1CO_2$ = 1 magnesite +$1H_2O$

20) 1 Brucite = 1 periclase + H_2O

Introduction of H_2O and small amounts of CO_2 results in the formation of rims of talc and magnesite around the serpentine. The talc and magnesite may then enclose pre-existing serpentine which formed in H_2O-rich environments alone (Winkler, 1974). If the X_{CO2} is not known, mineral parageneses formed in serpentines at higher temperatures do not constitute reliable temperature indicators (Winkler, 1974).

In the samples studied here, serpentine is closely associated with cracks in relict olivine grains and in some instances serpentine completely replaces the olivine grains pseudomorphically. Stringers of secondary magnetite are associated with this serpentine (Figure 5.21). Serpentine has also been found to be present as a rim around sulphide grains, with some of the needles penetrating into the sulphide grain. These serpentine rims have been found to have a talc halo, indicating a change in H_2O-CO_2 conditions (reaction 3).

XRD analyses indicate that amesite is the principal serpentine mineral present in the BGAB Unit. Amesite occurs as a metamorphic mineral in environments rich in Al, and its ideal formula is $(Mg_2Al)(SiAl)O_5(OH)_4$ (Deer et al., 1992). Amesite is chemically similar chlorite, but is structurally similar to serpentine with major substitution of Al for Mg and Si (Deer et al., 1992). According to Deer et al., (1992) there appears to be a complete solid solution range between serpentine and amesite due to this Al substitution. The average serpentine content of the BGAB Unit in this area is 3.7% (based on semi-quantitative XRD analyses).

Semi-quanitative XRD analyses show that detectable serpentine is not present in all samples of the LHZBG and PCR Units. These analyses indicate that lizardite is the principal

serpentine mineral in the LHZBG and PCR Units, with an average content of 3.8 and 5 % respectively.

Van Zyl (1996) indicates that microprobe analyses reveal serpentine from the Uitkomst Complex to have higher FeO and Al_2O_3 values than examples given by Deer et al., (1992) and ascribed it to the presence of chlorite on a sub-microscopically intermixed scale with the serpentine. It was also argued that the elevated levels of FeO may be due to a low oxygen fugacity and of a high SiO_2 activity during serpentinization. The serpentine (senso stricto) encountered in the present study was found only in the PCR Unit. The Al_2O_3 content of the serpentine in UK12 place it closer in composition to chrysotile, while the composition of the serpentine in UK61 place it close to Lizardite and that of UK48 to antigorite. The FeO content in all the samples were also found to be higher than values given by Deer et al., (1992).

The variation in composition of serpentine from the PCR Unit is shown in Table 5.4. The microprobe results and calculated formulas are presented in Appendix 2.

Table 5.4. The average composition of serpentine from the PCR Unit in different boreholes (n = number of grains analysed).

		Al_2O_3	FeO	MgO
UK12	Mean	0.14	2.73	40.94
	Std Dev	0.14	4.67	0.89
UK48	Mean	1.05	4.86	37.95
	Std Dev	0.52	0.49	0.53
UK61	Mean	0.74	6.07	37.12
	Std Dev	1.07	2.24	1.92

The Fe and Al content of the serpentine increases from the NW to the SE of the complex and the Mg content slightly decrease from the NW to the SE.

5.4 Secondary Magnetite

Secondary magnetite is found mainly as stringers in the internal cracks of preserved olivine grains. The secondary magnetite stringers are associated with serpentine in all cases (Figure

5.21). Secondary magnetite is also developed around primary chromite grains, in highly altered matrix material, mostly chlorite-talc assemblages in the PCR unit (Figure 5.22).

The mineral chemisty of the secondary magnetite grains encountered during this investigation, and obtained by microprobe analyses, is presented in Appendix 2. Summarized statistics of these analyses are presented in Table 5.5.

Table 5.5. Secondary magnetite grains from the PCR Unit.

n = 15	SiO_2	TiO_2	Al_2O_3	FeO	MnO	MgO	CaO	Na_2O	K_2O	Cr_2O_3	NiO
mean	0.34	0.04	0.03	87.78	0.03	0.22	0.17	0.01	0.01	0.08	0.05
std dev	0.54	0.03	0.04	1.29	0.02	0.49	0.56	0.01	0.01	0.14	0.05

n = number of analysis.

The alteration magnetite product around sulphide grains was not considered in the statistical evaluation, due to the difference in analytical set-up used as two different sets of standards, one for silicates and the second for sulphides and oxides, were used.

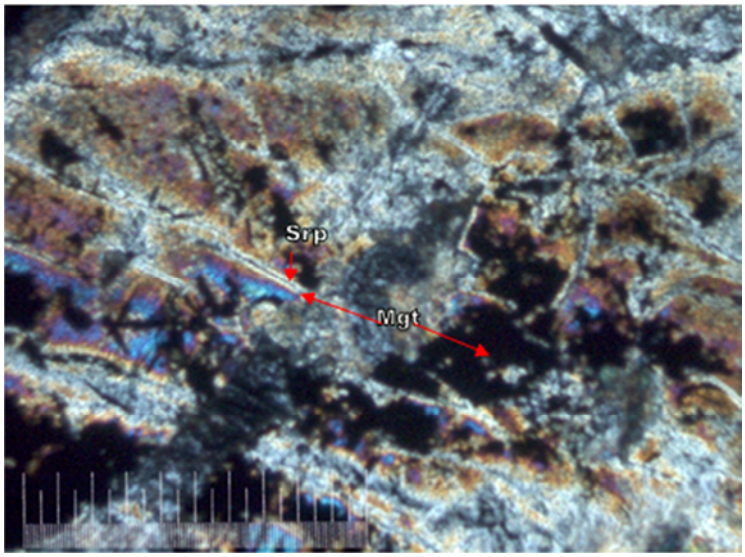

Figure 5.21. Magnetite (mgt) (black) occurring as non-continues stringers between serpentine (srp) visible in the grain on the left and almost completely pseudomorphically replacing olivine near the center of the picture. The picture scale bar is 1000 micron. Taken with cross-polarised light. (Sample: UK48C).

The formation of secondary magnetite stingers in the altered olivine grains are the product of topo-metasomatic mobilization of iron oxide from the olivine. It is suggested that this is the product of late-stage, low temperature hydrous retro-grade metamorphism.

In the case of secondary magnetite after primary magnetite, the association is with talc-dolomite assemblages in the PCR unit. This would suggest that alteration took place in an environment with higher CO_2-partial pressures. In most instances a core of relict chromite is preserved. No secondary magnetite after chromite were observed in the LHZBG Unit.

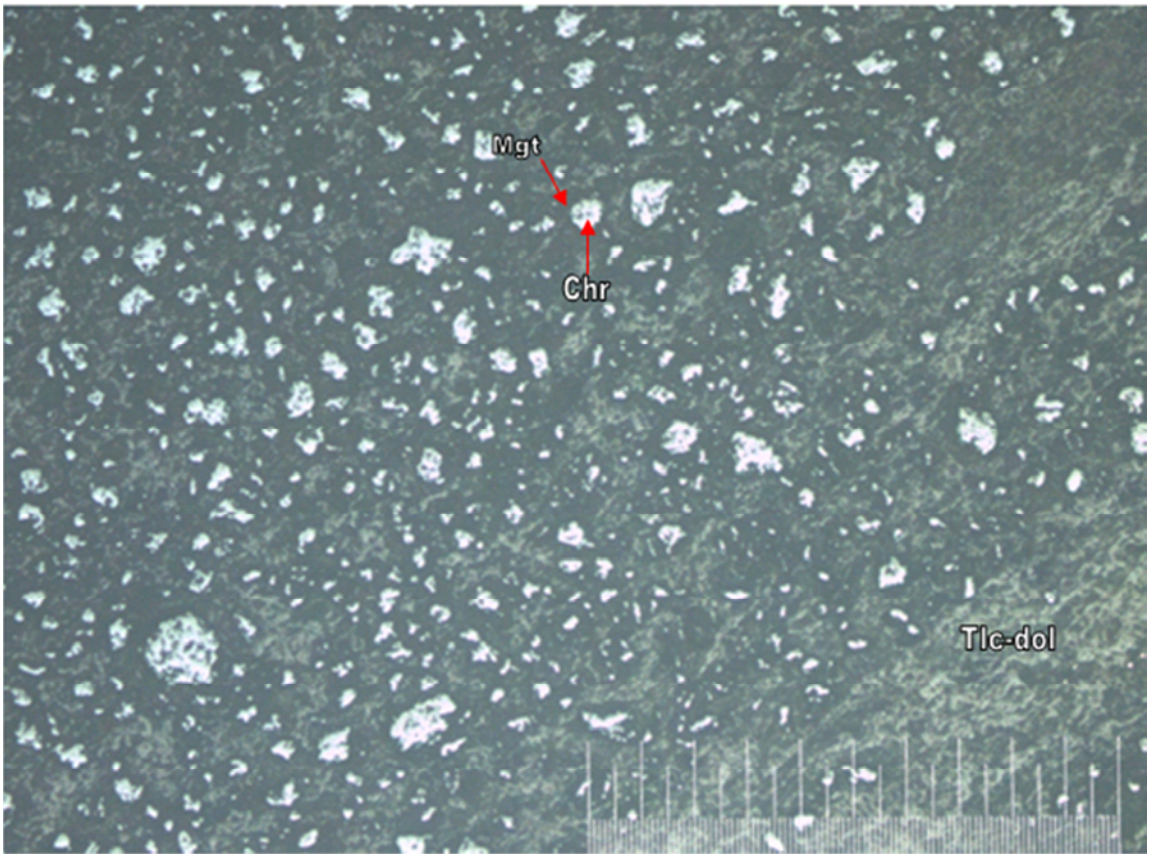

Figure 5.22. Chromite (chr) grains that show the effect of alteration. The chromite (white) grains are partly replaced by magnetite (gray) in a talc-dolomite (tlc-dol) matrix. The picture scale bar is 1000 micron. Taken with reflected light. (Sample; UK61C).

5.5 Talc

Microscopic investigation and microprobe analyses show that talc is closely associated with chlorite, phlogopite and amphiboles (Figure 5.23). Talc is also closely association with relic dolomite and pyrite grains that has the "orange skin-like" appearance (Figure 5.26). In various instances talc was found as part of a halo consisting of serpentine, talc and calcite around sulphide grains.

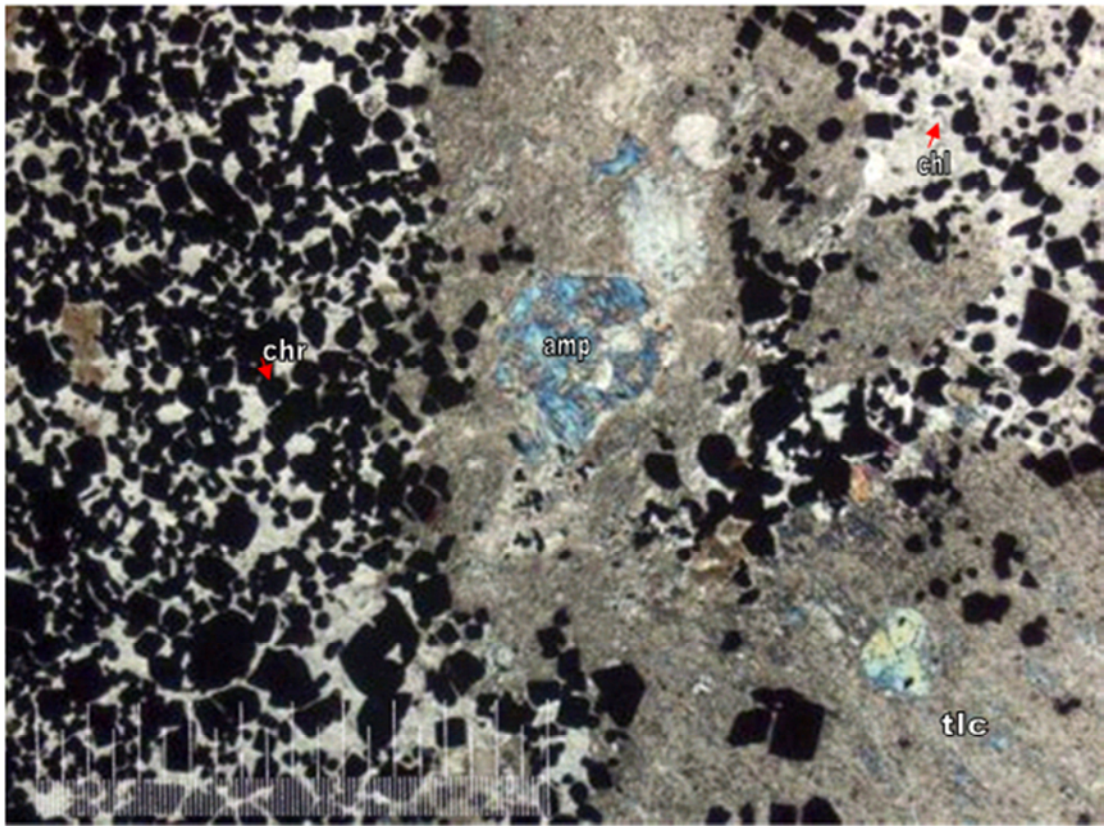

Figure 5.23. The alteration assemblage in the PCR, consisting of talc (tlc) (brown, low birefringence), chlorite (chl) (interstitial to chromite) and amphibole (amp) (high birefringence). Large to small euhedral chromite (chr) grains (black) are concentrated together. The picture scale bar is 1000 micron. Taken with cross-polarised light. (Sample: UK12A).

The occurrence of talc depends on the availability of sufficient Mg in the bulk rock composition. The paragenesis of talc can either be through low grade metamorphism (like hydrothermal alteration) of ultramafic rocks or by contact and regional metamorphism of

siliceous dolomites (Deer et al., 1992). However, the abundance of elements (Al, Ca and K) will favour the formation of minerals such as: Al = Chlorite, Ca = tremolite and K = phlogopite (Deer et al., 1992). In ultra-basic rocks talc is usually accompanied by serpentine and olivine forming lenticular veins (Deer et al., 1992).

Talc commonly forms at the expense of quartz and dolomite (Provoden et al., 2002). Steatization, the process through which serpentine is converted to talc is usually associated with serpentinization. During steatization talc is the main product with chlorite, serpentine and carbonates being accessories. Steatization may occur through the addition of silica and removal of magnesia, or by addition of CO_2.

$$2Mg_3Si_2(OH)_4 + 3CO_2 = Mg_3Si_4O_{10}(OH)_2 + 3MgCO_3 + 3H_2O$$

serpentine talc magnesite

At low temperatures both tremolite and chlorite may be converted to talc by CO_2 metasomatism. Talc is stable in the binary H_2O-CO_2 fluid up to X_{CO_2} of about 0.95. In the presence of magnesite, dolomite and calcite the stability of talc is progressively reduced to more restricted portions of the T-XCO_2 diagram.

If talc rather than tremolite is present, it implies that the X_{CO_2} of the original pore fluid was below 0.73 (Provoden et al., 2002). As H_2O is consumed and CO_2 produced, talc formation tends to shift the composition of the pore fluid along towards higher X_{CO_2} levels, this process results in internal buffering (Provoden et al., 2002). The reaction temperature for talc formation however varies significantly as a function of X_{CO_2} (Provoden et al., 2002).

The variation in composition of talc from the PCR and LHZBG Units is given in Table 5.6. The microprobe results and calculated formulas are presented in Appendix 2.

Table 5.6. Variation in composition of talc from the PCR and LHZBG Units (n = number of grains).

PCR		Al_2O_3	FeO	MgO
UK12	Mean	0.67	1.16	31.00
	Std Dev	0.46	0.10	0.54
UK48	Mean	1.08	4.02	29.16
	Std Dev	0.35	0.06	0.42
UK61	Mean	1.22	6.32	27.78
	Std Dev	1.49	1.84	0.95
LHZBG UK61	Mean	0.61	5.70	27.75
	Std Dev	0.74	1.72	1.32

The talc from UK12 in the PCR Unit and UK61 from the LHZBG Unit has a lower Al_2O_3 content relative to UK48 and 61 from the PCR Unit. The FeO content of talc in the PCR Unit intersected by UK12 is lower than in the PCR Unit intersection of UK48 and UK61 and than the talc within the LHZBG Unit intersected by UK61. The MgO content of all of the samples is fairly consistent. As these samples were collected from borehole closer to the inferred margin of the intrusion, the variation may be due to the variable degrees of assimilation.

Semi-quantitative XRD analyses shows that talc is virtually absent from the BGAG, while the talc content in the LHZBG and PCR Units are highly variable. Talc, however always attains its highest content in the PCR Unit.

5.6 Mica

The most common mica encounted during the present investigation is phlogopite. The ideal formula of phlogopite is $KMg_3AlSi_3O_{10}(OH)_2$ (Deer et al., 1992). Deer et al. (1992) noted that phlogopite occurs mainly in ultrabasic igneous rocks and particularly in kimberlites. Phlogopite and biotite are also found in metamorphic rocks that may form under a wide range of temperature and pressure conditions and phlogopite is common in metamorphosed pelites, basic and ultrabasic rocks, siliceous limestone and dolomite (Deer et al., 1992).

During this investigation phlogopite was encountered in the LHZBG and PCR Units. The phlogopite is usually found as part of the association talc-chlorite-phlogopite (Figure 5.24)

and in association with amphibole and carbonate. Phlogopite usually constitutes minor amounts of the investigated rock, but in sample UK32D of the PCR Unit, phlogopite and hornblende are the dominant minerals.

Figure 5.24. Phlogopite (brown) blade associated with talc and chlorite. The picture scale bar is 1000 micron. Taken with cross-polarized light. (Sample: UK48G).

Muscovite is generally present in the xenoliths of the LHZBG Unit. The muscovite occurs along with diopside, actinolite and chlorite in the "contaminated" variety of xenoliths. Muscovite and biotite is also found in the BGAB Unit. The muscovite in xenoliths from the LHZBG and BGAB Units is always associated with chlorite.

Microprobe analyses preformed on samples from the LHZBG and PCR units indicate the micas analysed to be phlogopite. The results are provided in Appendix 2 and summarized in Table 5.7 and 5.8.

Table 5.7. Average composition of phlogopite from the LHZBG Unit.

n=13	TiO_2	Al_2O_3	Cr_2O_3	FeO	MnO	MgO	CaO	Na_2O	K_2O	NiO
Mean	4.09	12.96	0.29	8.35	0.24	23.98	0.14	0.21	5.51	0.08
Std Dev	1.82	1.08	0.16	1.73	0.12	4.71	0.46	0.23	2.96	0.02

n = the number of analyses.

Table 5.8. Average composition of phlogopite from the PCR Unit.

n=21	TiO_2	Al_2O_3	Cr_2O_3	FeO	MnO	MgO	CaO	Na_2O	K_2O	NiO
Mean	3.41	13.40	0.72	6.68	0.04	24.39	0.01	0.14	6.59	0.06
Std Dev	2.66	0.47	0.48	2.95	0.03	5.49	0.03	0.15	2.98	0.03

n = the number of analyses.

Table 5.9. The Fe/Mg ratio of phlogopite from the LHZBG and PCR Units.

Fe/Mg	LHZBG	PCR
Minimum	0.19	0.12
Maximum	0.56	0.79
Average	0.37	0.31
Std Dev	0.15	0.20

No significant difference could be found between the compositions of phlogopite grains from in the LHZBG and PCR Units. The average Fe/Mg ratio of the analysed phlogopite grains (Table 5.12) show the ratio to be slightly higher in the LHZBG Unit compared to the PCR Unit. The calculated mineral formula for phlogopite is presented in Appendix 2.

5.7 Discussion

5.7.1. Growth of retrograde metamorphic mineral crystals

It has been noted that sulphide minerals in the LHZBG and PCR Units have been intergrown with fibrous minerals. It has been determined through optical and microprobe investigation that the majority of these minerals are actinolite-tremolite amphibole (Figure 5.25) and minor amounts of serpentine. The process which may have been responsible for this phenomenon is discussed in this section.

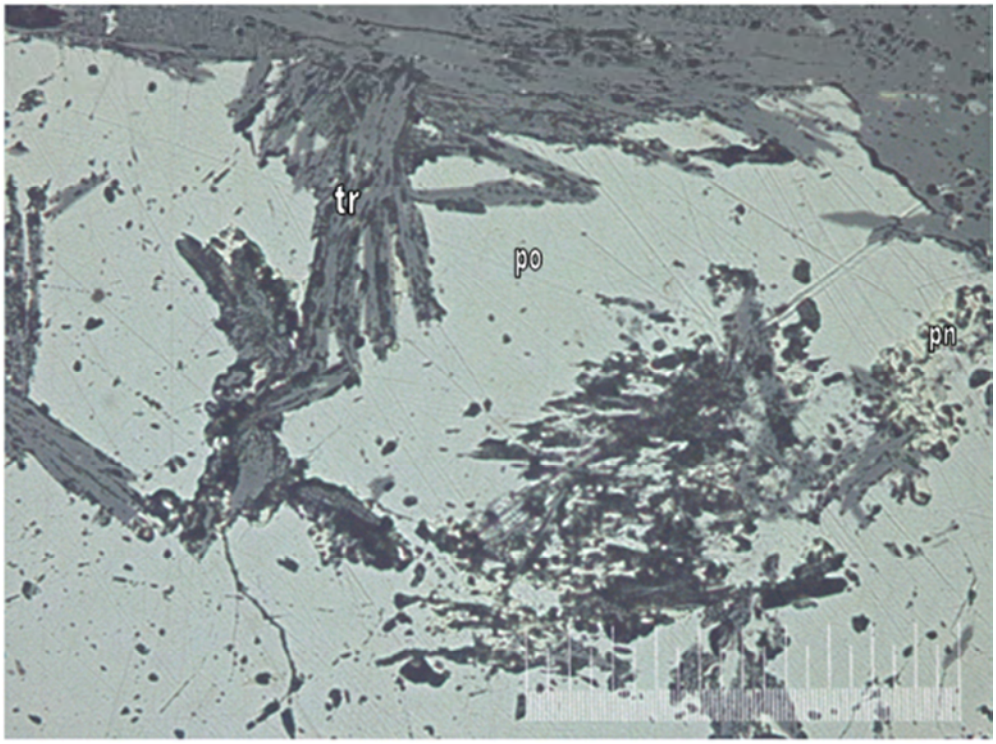

Figure 5.25. Granular pentlandite (pn) (light yellow) associated with tremolite (tr) blades (grey-black) intergrown with a pyrrhotite (po) grain (cream). The lines visible on the suface of the sulphide grain is due to poor polish. The picture scale bar is 1000 micron and it was taken with reflected light. (Sample; UK48L).

Secondary minerals intergrowths with sulphide grains have also been observed in the Stillwater Complex, Montana (Polovina et al., 2004). Here the sulphide grains have intergrowths of clinoziosite and Cl-rich ferropargasite, along with secondary sulphide minerals. This texture has been interpreted as representing a low temperature hydrothermal

event. Since secondary sulphides in association with the amphibole grains are absent in the Uitkomst Complex, a low temperature hydrothermal event, similar to that proposed for the Stillwater Complex is not considered.

Retrograde metamorphism happens where fluid and product minerals are in equilibrium during a mineral-fluid reaction (Ferry, 2000). This reaction will eventually lead to a state where the fluid and mineral products are in equilibrium with the mineral reactants. In the final stage where all of these are in local equilibrium, is assumed to give rise to the retrograde metamorphism, i.e. texture and assemblage. The mineral reactions during retrograde metamorphism will almost always involve carbonation or hydration.

Ferry (2000) indicates that one of the most distinctive features of retrograde metamorphism is the development of pseudomorphs. The pseudomorph will develop by the direct replacement of a reactant in a mineral reaction by one or more of the reaction products. In the case of a pseudomorph the outward crystal shape of the reactant will be preserved in the product. Ferry (2000) notes that pseudomorphs in prograde metamorphic reactions are relatively uncommon. Pseudomorphs are furthermore considered significant by Ferry (2000), as they records a novel phenomenon that results from the coupling of a chemical process, i.e. a mineral reaction, with a mechanical process and the force of crystallization during metamorphism. Force of crystallization is defined by Ferry (2000) as “the force exerted by a growing crystal against its surroundings, if those surroundings have finite yield strength”. He therefore suggests that force of crystallization will promote the formation of pseudomorphs during retrograde metamorphism.

It is suggested here that the actinolite-tremolite grains that are intergrown with the sulphide represent retrograde metamorphism of diopside grains. Possible multiple overprints of metamorphic events, coupled with hydrothermal fluids, will hamper any effort to empirically prove this relationship e.g. ratio of Ca:Fe:Mg in both due to possible different mobilization of elements in preserved diopside and actinolite-tremolite. It is however reasonable to suggest this particular primary to secondary mineral relationship. The

mechanism by which the diopside was transformed to actinolite-tremolite and the resultant growth into the spaces between discrete pentlandite and chalcopyrite is discussed in detail in the next section.

5.7.2. Retrograde metamorphism in the Uitkomst Complex

For the Uitkomst Complex, the most likely scenario of retrograde metamorphism envisaged is where the initial contamination of the magma responsible for the formation of the LHZBG and PCR Units caused the super saturation of sulphur resulting in the separation of an MSS phase. These MSS droplets accompanied by hydrous carbonate-rich fluids then accumulated interstitially to the semi-solid mush of silicate minerals. The MSS droplets may originally have been bordered by diopside that formed as an assimilation product in the contaminated magma. The diopside grains would then have been subjected to the effects of a carbonate-rich deuteric fluid that resulted in retrograde metamorphism of the diopside to actinolite-tremolite at the temperature where the MSS itself started crystallizing. The newly grown amphiboles of actinolite-tremolite composition then formed intergrowths with the last phases of the MSS to crystallize, namely the copper-rich phase.

The actinolite-tremolite grains probably suffered less resistance when crystallizing towards the sulphide grains and may have been able to slightly displace pentlandite when it encountered a fracture in the coarse grained pentlandite rims surrounding the main pyrrhotite grain. This would have resulted in the texture observed in Figure 5.6. The actinolite-tremolite grains may also have been able to mobilize some of the chalcopyrite rims surrounding the main pyrrhotite grains. The copper-rich MSS phase may have been relocated during growth of the actinolite-tremolite grains.

Pyrrhotite is not intergrown by the actinolite-tremolite grains. If the pyrrhotite crystallized out first from the MSS, it would have offered more resistance to growth than the non-cohesive coarse grained pentlandite or late phase chalcopyrite exsolution rims. The film on the surface of the growing actinolite-tremolite grain may then have been broken and expelled. The film may, as an alternative, have been retarded to such an extent that it was

not able propagate into the slightly harder pyrrhotite main grain. The well known hydrophobic character of sulphur may also have played a role if it may be assumed that fluid responsible for the retrograde metamorphism was hydrated. There may have been limited dissolution and recrystallization of the sulphide minerals, especially chalcopyrite, in the associated hydrothermal fluid. The effect was however limited and the magmatic disseminated texture were largely retained in the rock. However the possible interaction between the sulphide minerals and the solution that induced the growth of the actinolite-tremolite grains is beyond the scope of this investigation.

5.7.3. Petrogenetic significance of olivine

The lack of zoning in the olivine in addition to the high Ni content and Mg # of the olivine from both the LHZBG (including the wehrlite layers) and PCR Units indicate that the olivine is probably magmatic in origin. In the case of the LHZBG Unit it was not the result/product of metamorphism or metasomatism of siliceous dolomite, although the primary olivine grains probably equilibrated to variable degrees with the surrounding magma.

5.7.4. Petrogenetic significance of pyroxene

It is suggested that the diopside grains from the LHZBG Unit on the farm Slaaihoek 540 - JT, along with those in the wehrlite layers from within the PCR Unit represent clinopyroxene that crystallized from a magma that was less affected by assimilation of dolomitic country rocks. It may be inferred that the diopside in the PCR Unit is derived from a relatively uncontaminated magma, based on the petrographic descriptions and geochemical composition. The diopside grains from the LHZBG Unit on the farm Slaaihoek 540 - JT and from the wehrlite layers, are suggested to represent a mixture of diopside derived from primary magma and magma that assimilated some carbonate wall rocks. The greater similarity between the diopside grains from the LHZBG Unit on the farm Uitkomst 541 - JT and those within calc-silicate xenoliths may also indicate a greater degree of country rock assimilation by the magma in that area where the Complex widens. The grains showing a “transitional” feature between the two types of diopside may represent

clinopyroxene crystallizing from flows that suffered slightly less assimilation of country rock, possibly due to the formation of solidification fronts (discussed later in subsequent sections).

The differences in the composition of enstatite grains from the PCR Unit relative to enstatite grains from the wehrlite layers and LHZBG from the farm Slaaihoek may indicate a difference in either the magma composition between the two units, or a difference in crystallization environment, possibly due to differences in oxygen fugacity during the degassing of assimilating dolomite country rock. The higher Cr-content on the Slaaihoek section relative to the Uitkomst section indicates a more "primitive" composition, supporting the field evidence that intrusion of the conduit was from the northeast to the southwest.

5.7.5. Petrogenetic significance of plagioclase

It is suggested here that the near pristine plagioclase grains found in the LHZBG Unit were either in near equilibrium with the deuteric fluids that affected the surrounding precursor mafic minerals, or only suffered partial dissolution during the time it was exposed to the effects of the deuteric fluid. The resistance of the plagioclase, relative to its surrounding highly altered mineral matrix, is similar to that observed in the fassaite-diopside and phlogopite grains. This would suggest that a slight addition of an element to these minerals, not found in the surrounding matrix minerals, gives it an increased refractory property. In the light of the presence of fassaite-diopside it is suggested here that the accommodation of aluminium in their mineral structure is responsible for this property.The assimilation of Ca also resulted in the crystallization of clinopyroxene at the expense of orhtopyroxene and plagioclase. This is evidence of disruption of the original mafic magmatic composition.

5.7.6. Petrogenetic implications of chromite in the Uitkomst Complex

The formation of chromitite seams in magma chamber is not completely compatible with the formation of chromitite seams in a magma conduit. If it is assumed that a broadening of the magma conduit during the emplacement of further magma may in some respects

influence the physical conditions in a magma chamber, the formation of chromitite seams in the Uitkomst Complex may be explained in part. Two models are presented:

Firstly, it is suggested that the increase in oxygen fugacity in the Uitkomst Complex may be due to the assimilation of dolomite country rock (Gauert et al., 1996; Gauert, 1998) where CO_2 and H_2O may serve as agents for the precipitation of spinel (de Waal, 1977). It is suggested that the chromitite seams in the LHZBG Unit, but especially in the PCR and MCR Units may be due to the influx of fresh pulses of magma. These fresh pulses of primitive magma were then subjected to reaction with increased CO_2- and H_2O-enriched magma, resulting in periodic formation of chromite grains, that sank down to the top of the underlying cumulate mush to form a chromitite seam.

It is suggested here that the MCR Unit may have formed in reaction to the influx of the MHZBG magma over the residual PCR magma. The presence of chromitite seams in the MHZBG Unit may represent influxes of fresh magma into the conduit system, during the formation of the lower part of the unit, before the conduit system came to an end and development of the closed system.

It is further suggested that the more voluminous chromite mineralization in the SE relative to the NW part of the intrusion may have formed due to a sudden increase in oxygen fugacity in the south-eastern part of the Uitkomst Complex, where the intrusion broadens. The increase in oxygen fugacity in the south-eastern part of the intrusion relative to the north-western part of the intrusion may be due to the formation of reaction fronts and the direction of emplacement, namely from the north-west to the south-east. The combination of more rapid flow of magma in the narrow part, coupled with the development of reaction fronts (discussed in later sections) which prevented further degassing of the xenoliths and may have inhibited the settling of large amounts of chromite grains. The broadening of the intrusion on the Uitkomst section, leading to less rapid flow of magma and possible accumulation of CO_2-rich fluids and may have collectively led to an increase in oxygen fugacity as the magma flowed into this area. This resulted in the thicker chromite seams in

the Uitkomst section of the Complex. This decreased flow rate of the magma in the broader part of the Uitkomst Complex in the Uitkomst section, may have contributed to the settling out of the denser chromite crystals especially if a portion of the chromite grains, which settled out in this area, was initially carried in the streaming magma as suspension load.
The second model is based in part on the Stillwater Complex model proposed by Spadler et al. (2005). It is proposed that the magma that formed the PCR Unit was also responsible for the formation of the MHZBG Unit. As the magma stoped through the Rooihoogte sediments into the Timeball Hill shales, the magma began to interact with country rock richer in silica. This may have led to an increase in the amount of chromite crystallizing out of the system. As the conduit broadened, due to increased stoping of the shale country rock and a broadening of the conduit in the study area, the ability of the magma to suspend the chromitite load decreased. This would result in the formation of a thick layer of chromite at the base of the cumulate mush, represented by the PCR Unit. The result was the formation of the MCR layer. The subsequent formation of chromite stringers may indicate further stoping of the shales by the intruding magma, causing assimilation of the country rock, and thus formation of chromite grains, which would settle out on top of the cumulate mush present during that stage of development of the MHZBG Unit.

The absorption of CO_2-rich fluids in the Uitkomst magma may have been very limited. Most of the CO_2-rich fluids might have migrated upwards, and being trapped by the Massive Chromitite layer which served as a permeability barrier. These fluids would have been responsible for most of the alteration of the primary magmatic silicate minerals of the PCR Unit to a talc-chlorite-carbonate assemblage. Where the Massive Chromitite is not developed, especially in the NW, the CO_2-rich fluid was still able to stream or steam out of the system, resulting in the formation of the LrPRD Subunit. The chromite seams found in the LrPRD Subunit might be due to increased oxygen fugacity, caused by the influx of CO_2-rich fluids into the MHZBG Unit.

5.7.7. Petrogenetic significance of calcite

It is suggested here that the calcite encountered in the hybrid rocks represent the calcite melt forced out of the xenoliths, when the xenoliths suffered loss of volume and reacted with the magma. The calcite grains may have formed where the addition of Ca was not immediately accommodated by the magma or due to local cooling of a CO_2-rich fluid.

5.7.8. Petrogenetic significance of dolomite

Dolomite encountered in this investigation either forms part of the assemblage dolomite-talc-phlogopite or relic grains. It is encountered in minor amounts in both the PCR and LHZBG Units. The higher content of dolomite in some samples closer to the edge of the intrusion suggests that it may be derived from the dolomite country rock protruding into the Uitkomst Complex. An excess of dolomite that did not interact with the intruding magma appears to have survived the alteration processes affecting the Uitkomst Complex.

5.7.8 Petrogenetic implications of amphibole composition

It has been determined that the amphiboles were derived from a variety of metamorphic and or retrograde conditions. It is suggested that the "high-grade" amphiboles (e.g. edenite and magnesiohastingsite) may have crystallized out of trapped magmatic fluids that became enriched in volatiles. These amphiboles would thus have formed in a CO_2-rich environment that was not affected, or insignificantly affected by assimilation of the country rocks. These amphiboles may represent a "first generation" amphibole where it is found in the LHZBG Unit. In the PCR it may represent a remnant of the amphiboles associated with the original ultramafic rock, or as a product of metasomatic alteration of these ultramafic rocks.

The "lower-grade" amphiboles (e.g. tremolite and actinolite) are interpreted as being the result of retrograde metamorphism and metasomatic replacement of the precursor ultramafic minerals and hybrid rocks in an H_2O-enriched environment, where there might have been more extensive assimilation of country rock. The occurrence of actinolite-tremolite may be interpreted as resulting from retrograde metamorphism, as the actinolite-tremolite assemblage occur as pseudomorphs, and pseudomorphs are only present in retrograde metamorphic rocks (Ferry, 2000). These amphiboles may represent a "second generation"

of amphibole in especially the LHZBG Unit, where the "first generation" amphiboles or precursor clinopyroxene (diopside) may have been affected by hydrothermal alteration at lower temperatures. It may also represent the interaction product of an ultramafic magma with siliceous dolomite country rock in a H_2O-rich environment, especially where there is a close spatial association with calc-silicate xenoliths.

Sulphide mineralization is commonly associated with amphiboles of hornblende or magnesio-gedrite composition. Where the sulphide minerals are associated with these amphiboles, the contact between them tend to be sharp. Some sulphide grains are intergrown by amphiboles of a tremolite-actinolite composition. These amphiboles tend to only be intergrown with the chalcopyrite and pentlandite portions of the grain and not the main pyrrhotite grain. The origin of actinolite-tremolite is discussed in the following section. If it is accepted that the crystallization of the amphiboles requires an abundance of H_2O it may be inferred that the textural setting of the disseminated sulphide blebs are also associated with the same hydrous environment, especially the Cu-rich phase of the mono sulphide solid solution.

5.7.9. Petrogenetic significance of chlorite

The chlorite varieties occurring in the LHZBG Unit and in xenoliths from this unit have similar compositions and may reflect the same direct environment in which the hydrothermal event, responsible for the formation of the chlorite, took place. The Al and Fe-contents suggest a skarn as source, when compared to values given by Deer et al., (1992). In contrast, chlorite from the PCR contains less Fe and Mn but more Mg. This composition reinforces the fact that the alteration mineral assemblages in the PCR formed from an ultramafic igneous precursor.

The fact that chlorite occurs as pockets in amphibole may also indicate that the fluid responsible for the formation of chlorite passed through the rock at a later stage and possibly at a lower temperature than the fluid responsible for the formation of the amphibole. The fact that chlorite is not intergrown with the sulphide minerals also supports this hypothesis.

The close association of chlorite with especially talc and dolomite may indicate that the fluid was still carbonate-rich and deuteric.

It is also proposed here that at least two chlorite events affected the Uitkomst Complex. The first event is recorded by the chamosite after magmatic magnetite. The unusual preservation of the chamosite after magmatic magnetite was discussed earlier. It is considered unlikely that other remnants from this event would be persevered. The second event is recorded by the chlorite occurrence discussed in this section.

5.7.10. The petrogenetic significance of serpentine

Sakar, Ripley and Li, (2005) used oxygen and hydrogen isotopic analyses of samples from the Uitkomst Complex to determine that the fluids involved in the serpentinization process may have been of meteoric origin, but that the isotopic exchange occurred over a long period, at relatively low water/rock ratios. The evolved meteoric water stays in the country rock before mixing with later generated magmatic or hydrothermal water along the fluid path.

This implies that the hydrothermal alteration process, reflected in the samples collected, is responsible for the formation of the alteration assemblage minerals. Amongst others, the serpentine occurrences may have resulted from fluid derived by assimilation from the fluids present in the dolomite at the time of the intrusion. The assimilation of these fluids, rather than circulation of surface meteoric water, may be assumed to have been responsible for the formation of the serpentine in the fresh samples collected well below the limit of weathering and the current water table. The implication is that the initial fluid that resulted in the first alteration event may have been enriched in water derived from the assimilated dolomite country rock.

5.7.11 Petrogenetic significance of talc

It is suggested that the talc found in the PCR Unit represents the low grade retrograde hydrothermal alteration of the ultramafic rock by a carbonate-rich deuteric fluid. As talc

always attain it highest content in the PCR Unit, it may be inferred that the effects of this carbonate-rich deuteric fluid was more pervasive in this unit.

The occurrence of talc in the LHZBG Unit may also suggest the presence of a carbonate-rich deuteric fluid affecting the ultramafic rocks here, but that it was not as pervasive as in the PCR Unit. An alternative interpretation is that the origin of talc in the LHZBG Unit is related to contact metamorphism of the dolomitic country rocks rather than secondary alteration. This interpretation is supported by the occurrence of talc associated with dolomite and pyrite with an "orange skin" texture.

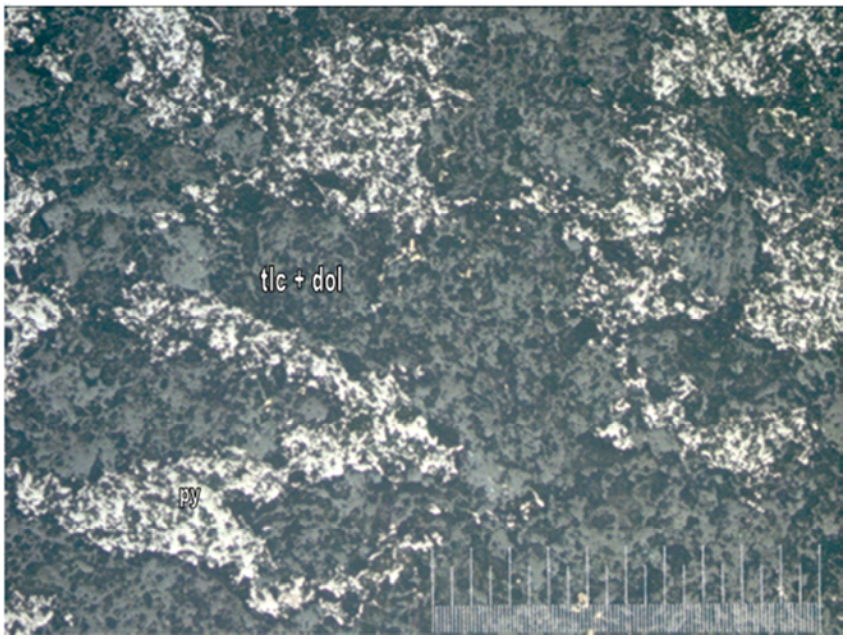

Figure 3.60. Anhedral pyrite (py) exhibiting a pitted "orange-skin" texture. The pyrite is found in a matrix of talc (tlc) and dolomite (dol). The picture scale bar is 1000 micron and it was taken with reflected light. (Sample; UK61F).

5.7.12 Petrogenetic significance of phlogopite and mica

Phlogopite and the occurrence of mica in the Uitkomst Complex is mainly associated with calc-silicate xenoliths and talc-dolomite assemblages. This would suggest that the mica and especially phlogopite minerals are the products of metamorphism of dolomitic country rock. This is demonstrated by the similar composition of the grains in the LHZBG and PCR. The

preservation of these grains and lack of over-printing, may as the case with plagioclase be, that the Al-content makes it more resistant to the effects retrograde metamorphism.

5.7.13 Petrogenetic significance of secondary magnetite

The stringers of secondary magnetite associated with olivine and serpentine would indicated the effect of a late-stage hydrous metasomatic event that affected both the LHZBG and PCR units. This event may be the same event that resulted in the formation of chlorite pockets in the these units. The secondary magnetite rims associated with chromitite grains in the PCR in the dolomite-talc assemblages may indicated that the fluid that led to the complete replacement of the precursor magmatic minerals affected the chromite grains, but did not completely replace it. All of these grains still have a chromite centre.